REPORT 1258

A WIND-TUNNEL TEST TECHNIQUE FOR MEASURING THE DYNAMIC ROTARY STABILITY DERIVATIVES AT SUBSONIC AND SUPERSONIC SPEEDS[1]

By BENJAMIN H. BEAM

SUMMARY

A method is described for measuring the dynamic stability derivatives of a model airplane in a wind tunnel. The characteristic features of this system are that single-degree-of-freedom oscillations were used to obtain combinations of rolling, yawing and pitching motions; that the oscillations were excited and controlled by velocity feedback which permitted operation under conditions unfavorable for more conventional types of oscillatory testing; and that data processing was greatly simplified by using analog computer elements in the strain-gage circuitry.

The system described is primarily for measurement of the damping derivatives C_{l_p} (damping in roll), $C_{m_q}+C_{m_{\dot{\alpha}}}$ (damping in pitch), $C_{n_r}-C_{n_{\dot{\beta}}}$ (damping in yaw), and the cross derivatives $C_{l_r}-C_{l_{\dot{\beta}}}$ (rolling moment due to yawing) and C_{n_p} (yawing moment due to rolling). The method of testing also permits measurement under oscillatory conditions of the static derivatives C_{l_β} (rolling moment due to sideslip), C_{n_β} (yawing moment due to sideslip), and C_{m_α} (pitching moment due to angle of attack). All these derivatives are of particular importance in estimating the short-period oscillatory motions of a rigid airplane.

A small number of experimental data are included to illustrate the general scope of results obtainable with this system.

INTRODUCTION

One important problem in the dynamic motions of airplanes is the nature and the stability of the oscillatory modes. In measuring the dynamic stability derivatives which apply to these motions there are certain advantages in employing oscillation methods in a wind tunnel, and the development of such methods has always been attractive to investigators. Most of the early measurements of damping in pitch were made from oscillation tests of a model in a wind tunnel. Damping in roll and damping in yaw have also been measured in this way but, in general, experimental difficulties have prevented the wide application of this method to the lateral motions. This is particularly true in the case of the cross derivatives, yawing moment due to rolling, and rolling moment due to yawing, although in one recently developed method (ref. 1) the yawing moment due to rolling has been successfully measured using a two-degree-of-freedom oscillatory technique.

Most of the studies of the lateral derivatives have been made on the basis of steady turning or rolling motions. Theoretical calculations of the derivatives are largely based on this assumption. The steady turning or rolling flow technique has been used in the systematic studies of the lateral derivatives in the Langley stability tunnel (e. g., refs. 2 and 3). Curved or rolling flight is approximated in the test section of this wind tunnel by causing the air to follow a curved or spiral path past a fixed model. At high speeds, the rolling derivatives have been measured by steadily rotating a sting-mounted model in a wind tunnel with a dynamometer and measuring the damping in roll, yawing moment due to rolling, and the side force due to rolling. These methods and other techniques have been described and referred to in various NACA publications on the stability derivatives for airplane and missile configurations.

The purpose of this report is to describe an oscillation technique for measuring the lateral and longitudinal dynamic stability derivatives in a wind tunnel. It was developed primarily for testing at high subsonic or supersonic speeds and for this reason three features are believed to be of special interest. One of these is the single-degree-of-freedom oscillatory system in which various components of pitch, roll, and yaw were obtained by varying the axis of oscillation. Second, the forcing system comprised a feedback loop in which velocity feedback was used to excite and control the amplitude of the model oscillation. A third feature is a system of strain-gage data processing in which electronic analog computer elements were used in measuring the amplitude and phase position of the oscillatory strain-gage deflections. The advice and assistance of the Ames instrument development branch was extremely valuable in developing this system of data processing.

The test apparatus is capable of measuring the moment derivatives which arise from angular motions of the airplane. This includes the rotary damping derivatives C_{l_p}, $C_{m_q}+C_{m_{\dot{\alpha}}}$, and $C_{n_r}-C_{n_{\dot{\beta}}}$; the cross derivatives C_{n_p} and $C_{l_r}-C_{l_{\dot{\beta}}}$; and the displacement derivatives C_{l_β}, C_{n_β}, and C_{m_α}. These derivatives are of particular importance in estimating the short-period oscillatory motions of a rigid airplane.

Two systems of axes are used in this analysis. The stability system of axes with the positive directions of moments and angles referred to this system are illustrated in figure 1. The oscillation axes used for wind-tunnel measurements

[1] Supersedes NACA TN 3347 entitled "A Wind-Tunnel Test Technique for Measuring the Dynamic Rotary Stability Derivatives Including the Cross Derivatives at High Mach Numbers," by Benjamin H. Beam, 1955.

are illustrated in figure 2 and defined with respect to the stability axes by a set of direction cosines. Primes are used with aerodynamic moment and axis designations referred to the oscillation system of axes.

The various stability derivatives are defined as follows:

$$C_{l_p} \quad \frac{2}{\rho V^2 Sb}\frac{\partial L}{\partial \frac{pb}{2V}} \qquad C_{l_{\dot\beta}} \quad \frac{2}{\rho V^2 Sb}\frac{\partial L}{\partial \frac{\dot\beta b}{2V}}$$

$$C_{n_p} \quad \frac{2}{\rho V^2 Sb}\frac{\partial N}{\partial \frac{pb}{2V}} \qquad C_{n_{\dot\beta}} \quad \frac{2}{\rho V^2 Sb}\frac{\partial N}{\partial \frac{\dot\beta b}{2V}}$$

$$C_{l_r} \quad \frac{2}{\rho V^2 Sb}\frac{\partial L}{\partial \frac{rb}{2V}} \qquad C_{l'_\sigma} \quad \frac{2}{\rho V^2 Sb}\frac{\partial L'}{\partial \sigma}$$

$$C_{n_r} \quad \frac{2}{\rho V^2 Sb}\frac{\partial N}{\partial \frac{rb}{2V}} \qquad C_{m'_\sigma} \quad \frac{2}{\rho V^2 Sb}\frac{\partial M'}{\partial \sigma}$$

$$C_{m_q} \quad \frac{2}{\rho V^2 S\bar c}\frac{\partial M}{\partial \frac{q\bar c}{2V}} \qquad C_{n'_\sigma} \quad \frac{2}{\rho V^2 Sb}\frac{\partial N'}{\partial \sigma}$$

$$C_{m_\alpha} \quad \frac{2}{\rho V^2 S\bar c}\frac{\partial M}{\partial \alpha} \qquad C_{l'_{\dot\sigma}} \quad \frac{2}{\rho V^2 Sb}\frac{\partial L'}{\partial \frac{\dot\sigma b}{2V}}$$

$$C_{m_{\dot\alpha}} \quad \frac{2}{\rho V^2 S\bar c}\frac{\partial M}{\partial \frac{\dot\alpha \bar c}{2V}} \qquad C_{m'_{\dot\sigma}} \quad \frac{2}{\rho V^2 Sb}\frac{\partial M'}{\partial \frac{\dot\sigma b}{2V}}$$

$$C_{l_\beta} \quad \frac{2}{\rho V^2 Sb}\frac{\partial L}{\partial \beta}$$

$$C_{n'_{\dot\sigma}} \quad \frac{2}{\rho V^2 Sb}\frac{\partial N'}{\partial \frac{\dot\sigma b}{2V}}$$

$$C_{n_\beta} \quad \frac{2}{\rho V^2 Sb}\frac{\partial N}{\partial \beta}$$

The following symbols are used in the report:

$A, B, * * *, H, J$	direction cosines between primed and unprimed axes
I	moment or product of inertia, depending on subscript, positive where negative moment results from positive acceleration, slug-ft²
K	mechanical spring constant, positive where negative moment results from positive deflection, ft-lb/radian
L	aerodynamic rolling moment, ft-lb
M	aerodynamic pitching moment, ft-lb
N	aerodynamic yawing moment, ft-lb
P	mechanical damping-moment coefficient, positive where negative moment results from positive velocity, ft-lb sec/radian
R	resistance, ohms
S	wing area, sq ft
T	torque, ft-lb
V	air velocity, ft/sec
b	wing span, ft
$\bar c$	mean aerodynamic chord, ft
e	voltage, volts
f	frequency of sinusoidal oscillation, cps
g	transfer function, $\frac{\text{output}}{\text{input}}$
i	galvanometer current, amp

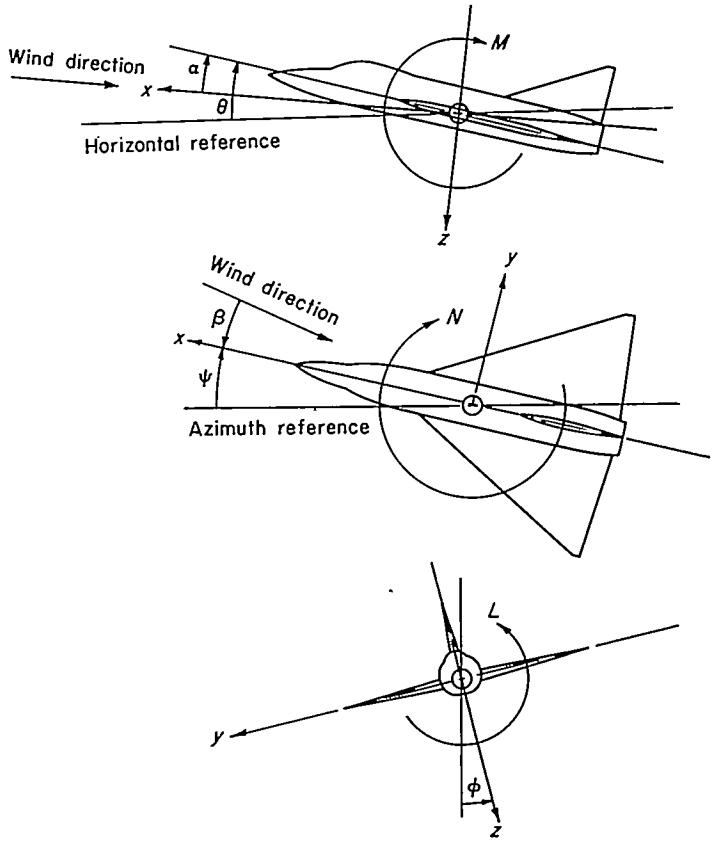

FIGURE 1.—The stability system of axes is an orthogonal system of axes having its origin at the center of gravity and in which the z axis is in the plane of symmetry and perpendicular to the relative wind, the x axis is in the plane of symmetry and perpendicular to the z axis, and the y axis is perpendicular to the plane of symmetry. Arrows indicate the positive directions of motions and moments.

k	strain-gage calibration constant, amp/volt/unit load
p	rolling velocity, radians/sec
q	pitching velocity, radians/sec
r	yawing velocity, radians/sec
t	time, sec
x, y, z	stability system of axes, defined in figure 1
x', y', z'	system of axes used for oscillation tests, defined with respect to the stability axes by the direction cosines
α	angle of attack, radians
α_m	mean or static angle of attack, deg
β	angle of sideslip, radians except where noted
θ	pitch angle, radians
φ	roll angle, radians
ψ	yaw angle, radians
σ	angle of rotation of model about x' axis, radians except where noted
ϵ	small angular displacement about y' or z' axis, radians
η, λ	direction angles, defined in figure 2, deg
μ, ν, ξ	phase angles of σ, T_x', and ϵ_y' with respect to an arbitrary reference
ρ	air density, slugs/cu ft
ω	circular frequency of oscillation, $2\pi f$, radians/sec

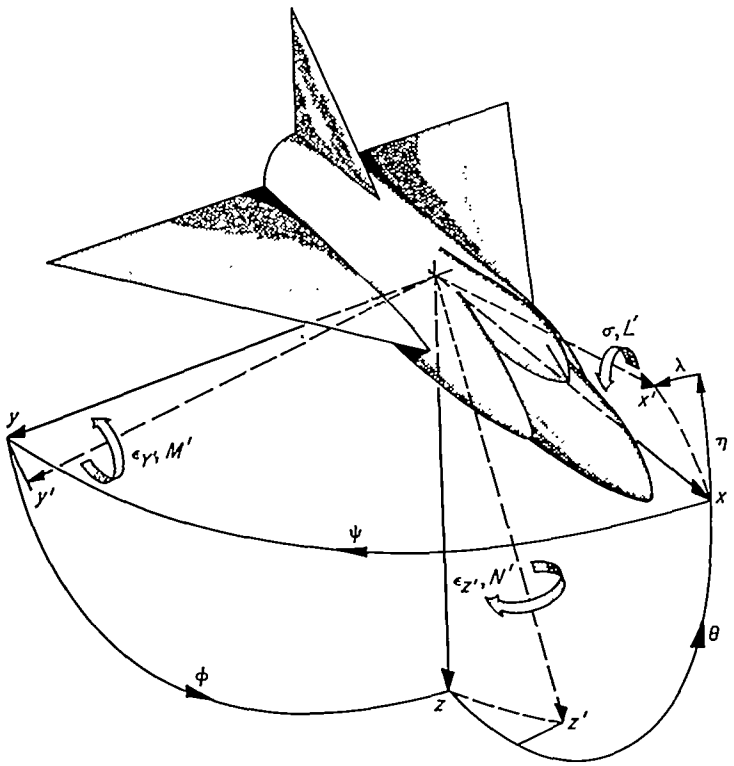

FIGURE 2.—The orientation of the oscillation axes, the x', y', z' system, is obtained by assuming an orthogonal system which is originally coincident with the stability system at zero angle of attack and with the same positive directions for forces, moments, and motions as being successively rotated about the y axis by an angle η and the x axis by an angle λ.

ω_o wind-off circular frequency of oscillations, radians/sec

$(\dot{})$ $\frac{d(\ )}{dt}$

$(\ddot{})$ $\frac{d^2(\ )}{dt^2}$

$\bar{(\ )}$ maximum value of a sinusoidally oscillating quantity $(\ )$

$\Delta(\ )$ incremental value of a quantity $(\ )$

Subscripts define the particular axis or motion to which the general symbol applies.

THEORY

SINGLE-DEGREE-OF-FREEDOM OSCILLATORY SYSTEM

The general dynamic motion of a rigid airplane with no moving control surfaces requires six differential equations. Three of these define translation and three define rotation about the center of gravity. If the center of gravity of a model airplane is fixed in a wind tunnel, the equations involving translation can be eliminated and the motion is defined in terms of rotary motions and derivatives by three equations. The system can be further restrained so that rotation occurs about one arbitrary fixed axis only. In this case the motion is defined by one equation even though simultaneous rolling, pitching, and yawing motions may be involved.

Assume an orthogonal coordinate system, the $x'y'z'$ system (fig. 2), the origin of which is at the center of gravity of the model airplane and in which rotation of the model is always about the x' axis. Equilibrium requires that the summation of the moments about the x', y', and z' axes be equal to zero. The equation for small angular oscillations about a static equilibrium condition can be written in terms of a single variable

$$-I_{x'x'}\ddot{\sigma}-P_{x'}\dot{\sigma}-K_{x'}\sigma+\Delta L'+T_{x'}=0 \tag{1}$$

The sign convention of figure 2 requires that if $I_{x'x'}$, $P_{x'}$, and $K_{x'}$ are considered positive quantities, their respective moments must be prefixed by a negative sign since they oppose the motion. The quantity $\Delta L'$ is the sum of all aerodynamic moments about the axis of oscillation arising from angular deflection, velocity, acceleration, etc., about the static equilibrium condition. The aerodynamic moments due to angular acceleration and higher-order terms are generally neglected in stability calculations. permitting the assumption that

$$\Delta L'=\frac{\partial L'}{\partial \sigma}\sigma+\frac{\partial L'}{\partial \dot{\sigma}}\dot{\sigma} \tag{2}$$

$$=\frac{1}{2}\rho V^2 Sb\left(\frac{b}{2V}C_{l'_{\dot{\sigma}}}\dot{\sigma}+C_{l'_\sigma}\sigma\right) \tag{3}$$

and equation (1) could be written

$$I_{x'x'}\ddot{\sigma}+\left(P_{x'}-\frac{1}{4}\rho VSb^2C_{l'_{\dot{\sigma}}}\right)\dot{\sigma}+\left(K_{x'}-\frac{1}{2}\rho V^2SbC_{l'_\sigma}\right)\sigma=T_{x'} \tag{4}$$

It is apparent from the left-hand side of equation (4) that $C_{l'_{\dot{\sigma}}}$ is an aerodynamic damping coefficient and that a negative value of $C_{l'_{\dot{\sigma}}}$ would result in a positively damped oscillation. A negative value of the coefficient $C_{l'_\sigma}$ would result in a positive restoring moment about the axis of oscillation. The sign convention is thus parallel to that of the stability derivatives about the stability axes.

Equations expressing the equilibrium of moments about the y' and z' axes for small oscillations about the x' axis can also be written

$$-I_{x'y'}\ddot{\sigma}+\Delta M'-K_{y'}\epsilon_{y'}=0 \tag{5}$$

$$-I_{x'z'}\ddot{\sigma}+\Delta N'-K_{z'}\epsilon_{z'}=0 \tag{6}$$

Equations (5) and (6) can be written in this simple form only if $\epsilon_{y'}$ and $\epsilon_{z'}$ are sufficiently small compared with σ that their effects are negligible in equations (1), (5), and (6) except for the terms $K_{y'}\epsilon_{y'}$ and $K_{z'}\epsilon_{z'}$. This is accomplished by limiting $\epsilon_{y'}$ and $\epsilon_{z'}$ to very small values but making $K_{y'}$ and $K_{z'}$ very large. In other words, the model would be relatively easy to deflect about the x' axis but very stiff about the y' and z' axes. From a development similar to that of equations (3) and (4) it can be shown that

$$-I_{x'y'}\ddot{\sigma}+\frac{1}{2}\rho V^2Sb\left(\frac{b}{2V}C_{m'_{\dot{\sigma}}}\dot{\sigma}+C_{m'_\sigma}\sigma\right)=K_{y'}\epsilon_{y'} \tag{7}$$

$$-I_{x'z'}\ddot{\sigma}+\frac{1}{2}\rho V^2Sb\left(\frac{b}{2V}C_{n'_{\dot{\sigma}}}\dot{\sigma}+C_{n'_\sigma}\sigma\right)=K_{z'}\epsilon_{z'} \tag{8}$$

The values of the aerodynamic coefficients in equations (4), (7), and (8) will change with the orientation of the oscillation axes in the wind tunnel and the attitude of the model with respect to the air stream. These changes are related to

changes in magnitude and relative contribution of the stability derivatives, ordinarily measured about the stability axes defined in figure 1. The geometric relation between the oscillation system of axes (the $x'y'z'$ system) and the stability axes (the xyz system) is completely defined by tne direction cosines between the two systems. These can be symbolized in the following matrix form

	x'	y'	z'
x	A	D	G
y	B	E	H
z	C	F	J

(9)

where, for example, the cosine of the angle between the y and z' axes is H.

The numerical evaluation of these direction cosines is somewhat complicated since the stability axes do not remain fixed with respect to the oscillation axes as the angle of attack is changed, as is apparent from a study of figures 1 and 2. It will be shown later in the appendix that certain simplifications are possible in numerical calculations by a less direct approach through a set of model axes. Since, however, in the present discussion the direction cosines are considered only in symbolic form, it is not necessary to introduce this additional step.

Small angular motions about the axis of oscillation can be resolved into component motions of roll, pitch, and yaw about the stability axes. The relative magnitude of each component depends on the direction cosine between the x' axis and the roll, pitch, or yaw axes, and, with the approximations sin $\sigma=\sigma$, cosine $\sigma=1$

$$\left.\begin{aligned} \Delta\varphi&=A\sigma & \dot{\varphi}&=p=A\dot{\sigma}\\ \Delta\theta&=B\sigma & \dot{\theta}&=q=B\dot{\sigma}\\ \Delta\psi&=C\sigma & \dot{\psi}&=r=C\dot{\sigma} \end{aligned}\right\} \tag{10}$$

The moments about the stability axes can be expressed in terms of the aerodynamic stability derivatives

$$\Delta L=\frac{1}{2}\rho V^2Sb\left[\frac{b}{2V}\left(C_{l_p}\dot{\varphi}+C_{l_r}\dot{\psi}+C_{l_{\dot{\beta}}}\dot{\beta}\right)+C_{l_\beta}(\Delta\beta)\right] \tag{11}$$

$$\Delta M=\frac{1}{2}\rho V^2S\bar{c}\left[\frac{\bar{c}}{2V}\left(C_{m_q}\dot{\theta}+C_{m_{\dot{\alpha}}}\dot{\alpha}\right)+C_{m_\alpha}(\Delta\alpha)\right] \tag{12}$$

$$\Delta N=\frac{1}{2}\rho V^2Sb\left[\frac{b}{2V}\left(C_{n_p}\dot{\varphi}+C_{n_r}\dot{\psi}+C_{n_{\dot{\beta}}}\dot{\beta}\right)+C_{n_\beta}(\Delta\beta)\right] \tag{13}$$

For straight flight, as in the wind tunnel, $\alpha=\theta$ and $\beta=-\psi$. The aerodynamic moments can then be referred back to the oscillation system of axes through the direction cosines.

$$\Delta L'=A(\Delta L)+B(\Delta M)+C(\Delta N) \tag{14}$$

$$\Delta M'=D(\Delta L)+E(\Delta M)+F(\Delta N) \tag{15}$$

$$\Delta N'=G(\Delta L)+H(\Delta M)+J(\Delta N) \tag{16}$$

Thus, the aerodynamic moments indicated in equations (1), (5), and (6) for oscillation about an arbitrary axis are defined in terms of moments about the stability axes by equations (14), (15), and (16). The aerodynamic coefficients which depend on the angular velocity of the model can be derived in terms of the stability derivatives as

$$C_{l'_{\dot{\sigma}}}=\frac{2}{\rho V^2Sb}\frac{\partial L'}{\partial\frac{\dot{\sigma}b}{2V}}=A^2C_{l_p}+AC\left(C_{n_p}+C_{l_r}-C_{l_{\dot{\beta}}}\right)+B^2\frac{\bar{c}^2}{b^2}\left(C_{m_q}+C_{m_{\dot{\alpha}}}\right)+C^2\left(C_{n_r}-C_{n_{\dot{\beta}}}\right) \tag{17}$$

$$C_{m'_{\dot{\sigma}}}=ADC_{l_p}+CD\left(C_{l_r}-C_{l_{\dot{\beta}}}\right)+EB\frac{\bar{c}^2}{b^2}\left(C_{m_q}+C_{m_{\dot{\alpha}}}\right)+AFC_{n_p}+FC\left(C_{n_r}-C_{n_{\dot{\beta}}}\right) \tag{18}$$

$$C_{n'_{\dot{\sigma}}}=AGC_{l_p}+CG\left(C_{l_r}-C_{l_{\dot{\beta}}}\right)+HB\frac{\bar{c}^2}{b^2}\left(C_{m_q}+C_{m_{\dot{\alpha}}}\right)+AJC_{n_p}+CJ\left(C_{n_r}-C_{n_{\dot{\beta}}}\right) \tag{19}$$

Those coefficients which depend on displacement of the model become

$$C_{l'_\sigma}=\frac{2}{\rho V^2Sb}\frac{\partial L'}{\partial\sigma}=-ACC_{l_\beta}+B^2\frac{\bar{c}}{b}C_{m_\alpha}-C^2C_{n_\beta} \tag{20}$$

$$C_{m'_\sigma}=-DCC_{l_\beta}+EB\frac{\bar{c}}{b}C_{m_\alpha}-FCC_{n_\beta} \tag{21}$$

$$C_{n'_\sigma}=-GCC_{l_\beta}+HB\frac{\bar{c}}{b}C_{m_\alpha}-JCC_{n_\beta} \tag{22}$$

In equation (17) $C_{l'_{\dot{\sigma}}}$ is the aerodynamic damping coefficient measured about the axis of oscillation in the wind tunnel. If the x' axis coincides with the x axis, the oscillation would be pure roll. In this case $A^2=1$ and $AC=B^2=C^2=0$ so the measured damping coefficient would be C_{l_p}, the damping-in-roll coefficient. Similarly, a pure pitching or yawing oscillation would result in the measurement of damping in pitch or damping in yaw.

In general, one stability derivative can be obtained from each separate physical measurement. In equations (17), (18), and (19) there are eight stability derivatives which depend on angular velocity; however, these derivatives form only five independent terms. The derivative C_{m_q} always appears with $C_{m_{\dot{\alpha}}}$ in the above since, for the pure rotary motions considered, q is always equal to $\dot{\alpha}$. (See ref. 4.) Similarly, since $r=-\dot{\beta}$ in a test of this type, $C_{l_r}-C_{l_{\dot{\beta}}}$ appears as one term and $C_{n_r}-C_{n_{\dot{\beta}}}$ as another. The evaluation of these five terms (C_{l_p}, C_{n_p}, $C_{m_q}+C_{m_{\dot{\alpha}}}$, $C_{l_r}-C_{l_{\dot{\beta}}}$, and $C_{n_r}-C_{n_{\dot{\beta}}}$) requires five unique measurements.

Equations (17), (18), and (19) can be considered in a purely formal way as the basis for a system of equations containing the unknown stability derivatives. Assuming that five values of $C_{l'_{\dot{\sigma}}}$, $C_{m'_{\dot{\sigma}}}$, or $C_{n'_{\dot{\sigma}}}$ are available from wind-tunnel measurements, along with the appropriate direction cosines for the axes about which the measurements were

made, a system of five equations could be formed. These equations could then be solved simultaneously for the five stability derivatives, providing the equations are mathematically determinate.

The necessary values of $C_{l'_{\dot\sigma}}$, $C_{m'_{\dot\sigma}}$, or $C_{n'_{\dot\sigma}}$ which lead to the velocity derivatives and $C_{l'_\sigma}$, $C_{m'_\sigma}$, or $C_{n'_\sigma}$ which lead to the static derivatives are obtained from physical measurements of the model oscillation through equations (4), (7), and (8). Measurements can be made of the frequency of oscillation ω, the input torque $T_{x'}$, the oscillation amplitude σ, and the small angular deflections $\epsilon_{y'}$ and $\epsilon_{z'}$. There is considerable latitude in the choice of axes of oscillation and the particular quantities to be measured within the general confines of mathematical determinateness of the stability derivatives. Note, however, that $\epsilon_{y'}$ and $\epsilon_{z'}$ are inherently more difficult to measure than σ. The small displacements and high stiffness required about the y' and z' axes to maintain the validity of equations (4), (7), and (8) impose a limitation on the accuracy of measurements about these axes. Friction, backlash, and interaction become of increasing importance as the displacement is reduced. Some measurements must be made in conjunction with large static pitching moments or aerodynamic disturbances of a random nature and these factors will affect the design of the apparatus and the accuracy of the system. These factors, and the methods used to relate the measurements of $T_{x'}$, ω, σ, $\epsilon_{y'}$ and $\epsilon_{z'}$ to the derivatives $C_{l'_{\dot\sigma}}$, $C_{n'_{\dot\sigma}}$, etc., are discussed in subsequent sections. The direction cosines which relate the derivatives $C_{l'_{\dot\sigma}}$, $C_{n'_{\dot\sigma}}$, etc., to the various stability derivatives in equations (17) through (22) are given in the appendix.

FEEDBACK CONTROL

As indicated in the preceding section, measurement of the aerodynamic derivatives depends upon an analysis of a single-degree-of-freedom oscillation defined by equation (4) repeated here for convenience.

$$I_{x'x'}\ddot\sigma+\left(P_{x'}-\frac{1}{4}\rho VSb^2C_{l'_{\dot\sigma}}\right)\dot\sigma+\left(K_{x'}-\frac{1}{2}\rho V^2SbC_{l'_\sigma}\right)\sigma=T_{x'} \tag{4}$$

In the case of a free oscillation $T_{x'}$ would become zero and the oscillation would be a damped sinusoid. Use of this method is generally limited to test conditions which would not result in oscillatory instability as there is no control over the amplitude once the oscillation is initiated.

For the forced oscillation $T_{x'}$ in equation (4) is a sinusoidal function of time. One case of interest is where the frequency of the applied torque corresponds to the undamped natural frequency of the oscillatory system. At this frequency the inertia moments balance the restoring moments and the final amplitude after the decay of initial transients corresponds to a balance between the damping moments and the applied torque. The maximum angular velocity of oscillation can be obtained with a minimum of input torque at this frequency, as the entire input is used to overcome the damping. It is thus a desirable operating point both from the standpoint of power requirements and accuracy in measuring the damping.

One disadvantage with the forced-oscillation system operating at the resonant frequency is that, as with the free-oscillation system, testing cannot be conducted where oscillatory instability is encountered. At high Mach numbers and high angles of attack where minor changes in test conditions may produce changes in the aerodynamic derivatives, a steady-state oscillation is very difficult to maintain. In situations such as this, feedback control of the oscillation should be considered as it provides a means for automatically stabilizing the amplitude and the frequency of the oscillation for any variation of damping, either positive or negative, within the capacity of the forcing system.

The system of feedback control used in the present apparatus evolved from unsuccessful experiments with the forced-oscillation technique described above at high subsonic Mach numbers. After the development of the feedback system it was found that Bratt, Raymer, and Miles in England had used a similar technique in 1942 but the results of their experiments are not generally available. The principle of operation is similar to that of the amplitude-stabilized feedback oscillator.

The oscillatory system was formed by the moment of inertia of the model and the stiffness of the restoring springs. Torque was applied to this system in the present case through a linkage with an electromagnetic shaker. It is convenient to think of the shaker system as a transducer which converts an electrical signal input into a torque. A strain gage indicating the angular deflection of the model converted the oscillation amplitude into an electrical signal. Feedback was accomplished by using amplified voltage from the strain gage as a source of electrical signal to the shaker. Velocity feedback was used in this case and the strain-gage signal of oscillation amplitude was differentiated electronically before being introduced into the shaker.

Thus, for a system with velocity feedback

$$T_{x'}=g\dot\sigma \tag{23}$$

and equation (4) could be written

$$I_{x'x'}\ddot\sigma+\left(P_{x'}-\frac{1}{4}\rho VSb^2C_{l'_{\dot\sigma}}-g\right)\dot\sigma+\left(K_{x'}-\frac{1}{2}\rho V^2SbC_{l'_\sigma}\right)\sigma=0 \tag{24}$$

If g and the aerodynamic derivatives are constants, equation (24) is linear. The case of interest is where

$$P_{x'}-\frac{1}{4}\rho VSb^2C_{l'_{\dot\sigma}}-g=0 \tag{25}$$

In this case,

$$\sigma=\bar\sigma e^{j\omega t} \tag{26}$$

The oscillations are sinusoidal and of constant amplitude. The oscillation frequency is the undamped natural frequency, given by

$$\omega=\sqrt{\frac{K_{x'}-\frac{1}{2}\rho V^2SbC_{l'_\sigma}}{I_{x'x'}}} \tag{27}$$

The peak amplitude of the oscillation, $\bar\sigma$, cannot be defined independently of initial conditions if the terms in equation

(24) are constant as assumed. Amplitude stabilization would require that the final oscillation amplitude be independent of the initial conditions in the same sense that a "limit cycle" is independent of the starting conditions in a nonlinear oscillatory system. The transfer function, g, of the feedback loop can be designed to vary with oscillation amplitude in such a way as to produce positive feedback at low amplitudes and negative feedback at high amplitudes with a limit cycle at some intermediate amplitude. This type of stabilization, however, would appear to conflict with the requirement that g and the other coefficients in equation (24) be constants for sinusoidal motion. These conflicting requirements can be satisfied within practical limits by allowing g to vary with oscillation amplitude, but at such a slow rate that it remains essentially constant through one cycle of operation.

A rudimentary circuit of a quasi-linear element which could be inserted in the feedback loop to stabilize the amplitude of oscillation is shown schematically in figure 3 (a) along with a sketch of its transfer function, figure 3 (b). The thermister is the nonlinear control element. It is characterized by a high negative temperature coefficient of resistance and as current, either alternating or direct, is passed through it the resultant heating causes its resistance to change. The thermal and heat-transfer characteristics of the thermister determine the time required to reach a new resistance following a change in current. There are many variations of the principle illustrated in figure 3 which would produce an equivalent result and which can be found in the

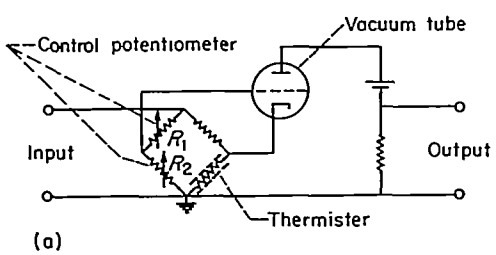

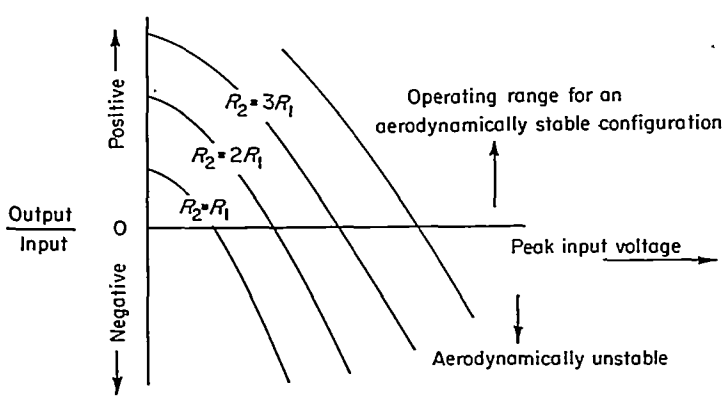

(a) Simplified schematic.
(b) Transfer function for several fixed positions of the control potentiometer.

FIGURE 3.—Simplified characteristics of the amplitude-control circuit.

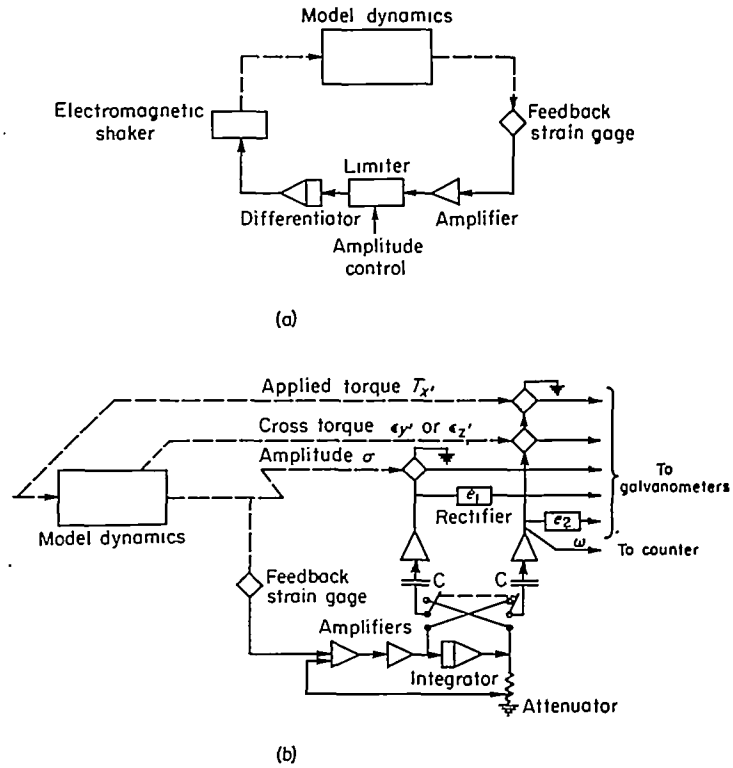

(a) Excitation system.
(b) Computing system.

FIGURE 4.—Block diagram of the excitation and computing systems

literature on amplitude stabilization of electronic oscillators.

A schematic diagram of the complete feedback control loop is shown in figure 4 (a). With this system the input torque, given by $g\dot{\sigma}$, can be made equal and opposite to the damping moments acting on the model for any value of $\bar{\sigma}$ by an adjustment of the potentiometer in figure 3 (a). For amplitudes less than the desired amplitude the damping moment will be less than the applied torque and oscillations will build up from rest. For amplitudes greater than desired, the damping moments will be greater than the applied torque and oscillations will decrease. The only stable operating point is where

$$P_{x'}-\frac{1}{4}\rho VSb^2C_{l'_{\dot{\sigma}}}-g=0 \tag{28}$$

and this can be shown to apply whether the aerodynamic damping is positive or negative.

ANALOG COMPUTING SYSTEM

By use of the feedback control system described, the static derivatives C_{m_α}, C_{n_β}, and C_{l_β} can be determined from equation (27) and an accurate measurement of the change in oscillation frequency between the wind-on and wind-off test conditions. The equation for $C_{l'_{\dot{\sigma}}}$ can be obtained from equation (27)

$$C_{l'_{\dot{\sigma}}}=\frac{-2K_{x'}}{\rho V^2Sb}\left[\left(\frac{\omega}{\omega_o}\right)^2-1\right] \tag{29}$$

Three values of $C_{l'_{\dot{\sigma}}}$ are required for different orientations of the axis of oscillation. Inserting these values into equation

(20) with the appropriate direction cosines provides three equations for the unknowns C_{m_α}, C_{n_β}, and C_{l_β}.

Measurement of the velocity derivatives is more difficult. Early attempts to record the output of strain gages with an oscillograph and then to measure the amplitude and phase position of each trace proved to be an expensive and time-consuming task even with the aid of automatic digital computing equipment. The analog computing system discussed herein performs the same mathematical processes as the digital computing machine, but does so at the time the data are taken and results in a considerable saving in the time and expense devoted to data processing.

The measurements required in this case for a determination of the velocity derivatives were σ, $T_{x'}$ and either $\epsilon_{y'}$ or $\epsilon_{z'}$. Each of these time-varying quantities can be represented as a Fourier series in ωt by the general expression

$$F(t)=a_0+a_1 \cos \omega t+b_1 \sin \omega t+ \ . \ . \ . \ a_n \cos n\omega t+b_n \sin n\omega t \tag{30}$$

where ω is the fundamental frequency of oscillation. Higher-order terms are always present to some degree because of buffeting of the model, wind-tunnel vibration, etc.; however, only the fundamental component in $F(t)$ is of interest. The amplitude and phase position of the fundamental can be determined from the Fourier coefficients, defined by

$$a_1=\frac{1}{\pi}\int_{-\pi}^{\pi} F(t) \cos \omega t \, d(\omega t) \tag{31}$$

$$b_1=\frac{1}{\pi}\int_{-\pi}^{\pi} F(t) \sin \omega t \, d(\omega t) \tag{32}$$

If strain-gage bridges are located in the oscillation apparatus in such a position as to indicate σ, $T_{x'}$, and $\epsilon_{y'}$, the output of each gage would be proportional to the product of applied voltage and gage deflection. Introducing a voltage into each gage of $\bar{e} \cos \omega t$ results in a gage output current of

$$i=k\bar{e}F(t) \cos \omega t \tag{33}$$

As in equation (30), ω is the fundamental frequency of oscillation so that upon expanding, equation (33) becomes

$$i=k\bar{e}\left(a_o \cos \omega t+\frac{a_1}{2}+\frac{a_1}{2} \cos 2\omega t+b_1 \sin \omega t \cos \omega t+ \ . \ . \ .\right) \tag{34}$$

A well-damped deflection galvanometer having a time constant much greater than $\frac{2\pi}{\omega}$ will not respond to currents of fundamental frequency and above. Its deflection will be proportional to the average galvanometer current, given by

$$i_{av}=\frac{1}{2\pi}\int_0^{2\pi} i \, d(\omega t) \tag{35}$$

With equations (34) and (35), an expression for a_1 can be obtained in terms of the average galvanometer current

$$a_1=\frac{2i_{av}}{k\bar{e}} \tag{36}$$

Wherein i_{av} and $\bar{e}$ can be measured directly at the time of the test and k can be obtained from a static calibration of the strain gage. Simularly, b_1 can be measured using a sine wave of voltage in place of a cosine wave. The 90° phase separation between the sine and cosine voltages was obtained in this case using the input and output, respectively, of an electronic integrator. This integrator and other active components in the computing circuitry consist essentially of high gain d-c amplifiers in which the input and feedback impedances to each amplifier determine its specific function. Similar components were used in the feedback loop described previously.

A schematic diagram of the computing system used is shown in figure 4(b). The signal source for the sine and cosine voltages was the strain gage, indicating oscillation amplitude, that was used to excite the feedback loop. The reversing switch was used to apply the sine and cosine voltages alternately to each gage. These voltages were measured simultaneously with each reading by means of the rectifier circuits e_1 and e_2 and the galvanometers. The feedback loop through the attenuator was used to suppress any unusually large variations in direct current through the integrator, and the capacitors prevented this direct current from appearing at the output.

The in-phase and out-of-phase components, a_1 and b_1, respectively, of $T_{x'}$, $\epsilon_{y'}$, $\epsilon_{z'}$, and σ are used to determine the maximum amplitude and relative phase position of each. Only the component of $T_{x'}$, $\epsilon_{y'}$, and $\epsilon_{z'}$ in quadrature with the amplitude is required to calculate the mechanical damping and the velocity derivatives. For example, with the notation

$$\sigma=\bar{\sigma} \sin (\omega t+\mu)$$

$$T_{x'}=\overline{T}_{x'} \sin (\omega t+\nu)$$

$$\epsilon_{y'}=\bar{\epsilon}_{y'} \sin (\omega t+\xi)$$

the velocity coefficients for each oscillation condition can be calculated from equations (4) and (7) as

$$C_{l_\sigma'}=\frac{4}{\rho VSb^2}\left[P_{x'}-\frac{\overline{T}_{x'} \sin (\nu-\mu)}{\omega\bar{\sigma}}\right] \tag{37}$$

$$C_{m_\sigma'}=\frac{4}{\rho VSb^2}\frac{K_{y'}\bar{\epsilon}_{y'}}{\omega\bar{\sigma}} \sin (\xi-\mu) \tag{38}$$

Four values of $C_{l_\sigma'}$ and one of $C_{m_\sigma'}$ were required in this case which, with equations (17) and (18), yielded the five rotary derivatives C_{l_p}, C_{n_p}, $C_{m_q}+C_{m_{\dot{\alpha}}}$, $C_{l_r}-C_{l_{\dot{\beta}}}$, and $C_{n_r}-C_{n_{\dot{\beta}}}$.

OPERATION

DESCRIPTION OF APPARATUS

The oscillation mechanism necessary for the dynamic tests was housed in a sting assembly which was matched to the dynamic model and the wind-tunnel model support in such a way that it was interchangeable with the stings normally used for static testing. It was thus possible to measure the static force and moment characteristics and the dynamic stability derivatives under identical test conditions.

FIGURE 5.—Model airplane installed on oscillation mechanism in wind-tunnel test section.

A model airplane mounted on the oscillation equipment in the wind tunnel is shown in the photograph, figure 5. An electromagnetic shaker was housed in the enlarged portion of the sting downstream of the model airplane. Special model construction was required to obtain the necessary strength with a minimum of weight since a reduction in weight simplified many of the other design problems, particularly those relating to the supporting springs. Designed for a wing loading at high Mach numbers of approximately 400 pounds per square foot, the weight of the model in figure 5 is approximately 5 pounds per square foot of wing area.

A general view of the electronic equipment needed outside the test section is shown in the photograph, figure 6. The console on the right in the photograph is the power supply for the electromagnetic shaker housed in the model supporting sting. The panel rack on the left contains a counter for measuring frequency and the various electronic feedback and computing elements illustrated in the block diagrams, figure 4. The galvanometer and read-out system, not shown in figure 6, is the same as that normally used for static tests with a strain-gage balance.

Two oscillation mechanisms were built, one for pure pitching or yawing oscillations in which the oscillation axis was perpendicular to the longitudinal axis of the supporting sting, and one for combined rolling and pitching or rolling and yawing in which the axis of oscillation was inclined 45° to the longitudinal axis of the sting. The essential features of these mechanisms are shown in figures 7, 8, and 9. The crossed flexure pivots position the model and provide the spring restraint for the oscillatory system. The axis at which the flexure pivots cross is the axis of oscillation. Several sets of flexure pivots of different thickness were provided which permitted testing at frequencies from approximately 3 to 10 cycles per second. Each of these mechanisms could be driven by a shaker with a reciprocating motion of the push rod.

The measurement of $\epsilon_{y'}$ and $\epsilon_{z'}$ required special consideration as these quantities are more difficult to measure than ω, $T_{x'}$, and σ because of the small deflections involved. An examination of equation (17) shows that all the stability derivatives which depend on angular velocity of the model influence the damping of the oscillation. The four groups of terms which appear in equation (17) can be resolved into measurements of ω, $T_{x'}$, and σ in a series of four tests in which all test conditions remain constant except for changes in orientation of the axis of oscillation. In other words, $C_{m_q}+C_{m_{\dot{\alpha}}}$, C_{l_p}, and $C_{n_r}-C_{n_{\dot{\beta}}}$ can be resolved by measurements of damping, but only the sum of the cross derivatives $C_{n_p}+C_{l_r}-C_{l_{\dot{\beta}}}$ can be determined in this manner. At least one additional measurement of $\epsilon_{y'}$ or $\epsilon_{z'}$, represented by equations (18) and (19), is required to resolve these two derivatives.

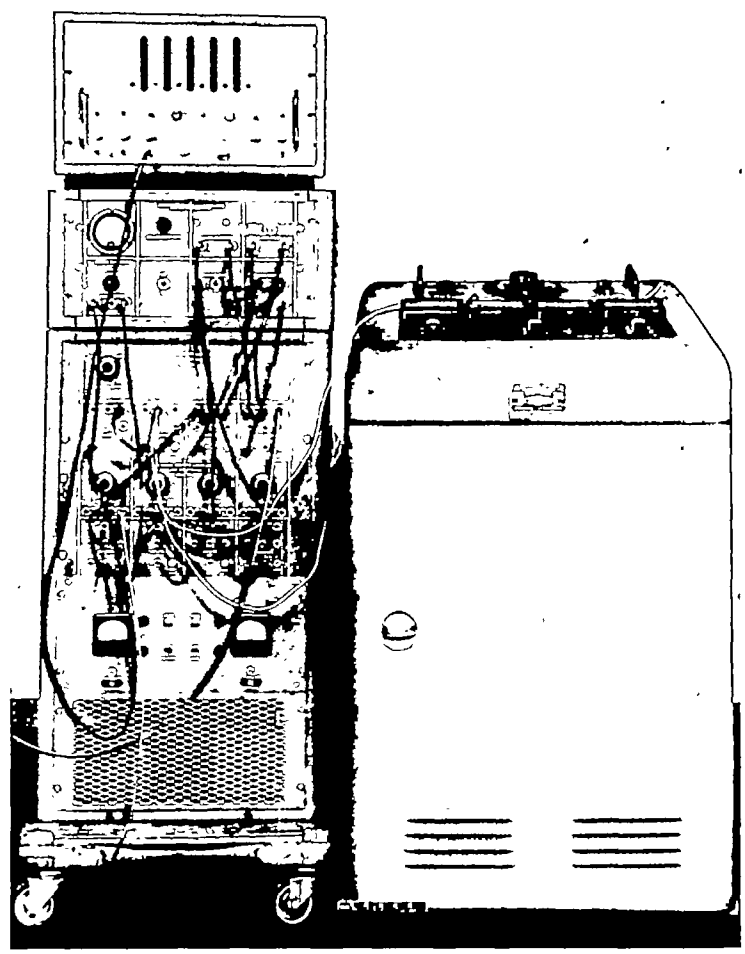

FIGURE 6.—General view of electronic feedback and computing equipment used for the oscillation tests.

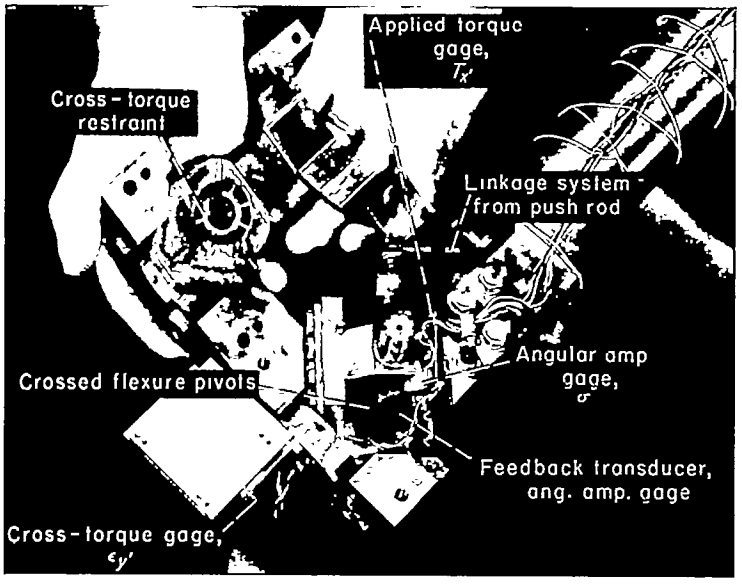

FIGURE 7.—Oscillation mechanism with oblique axes showing the cross-torque gage used in early tests.

Figure 7 represents an early version of the oscillation mechanism in which $\epsilon_{y'}$ was measured to obtain C_{n_p} in a rolling and pitching oscillation. Accuracy was expected to be a maximum here because moments due to other aerodynamic derivatives would have little effect on $\epsilon_{y'}$. This is apparent on substituting the direction cosines for a rolling and pitching oscillation from the appendix into equation (18). The strain gage indicating $\epsilon_{y'}$ was of the unbonded type since the angular deflection about the y' axis was ± 0.0005 radian or less. The deflection was held within the above limits by the radial flexures indicated as the cross-torque restraint in figure 7. This gage was used for testing only during rolling and pitching oscillations and was mechanically disconnected for other orientations.

This mechanical arrangement of the oscillation mechanism proved workable but experience gained over several months of wind-tunnel testing revealed some undesirable characteristics which could be corrected by redesign. One difficulty was due to an interaction between the cross torque and the applied torque. Analysis showed that deflections of the trunnion to which the crossed flexure pivots and the cross-torque restraint were attached could result in an indicated $\epsilon_{y'}$. It was established from a static calibration that approximately 6 percent of a moment about the x' axis was measured as a moment about the y' axis because of this interaction, and thus a correction to the measured values of $C_{m'_\sigma}$ was necessary which amounted to approximately 6 percent of the measured values of $C_{l'_\sigma}$.

One other difficulty with this system was due to unbalanced static aerodynamic moments, which do not appear in the dynamic equations because they remain constant, but which are also supported by the mechanism. The largest of these moments is normally the pitching moment, and the range of angles of attack for testing in the pitching mode is thus limited by the permissible angular deflection of the flexure pivots caused by the static pitching moment. It is seen that the cross derivative C_{n_p} is measured in a combined rolling and pitching mode in which the test range of angles of attack is limited by these conditions; whereas the remaining lateral-directional derivatives are measured in a rolling and yawing mode or in a pure yawing mode and are thus not limited in angle-of-attack range by aerodynamic pitching moments.

A consideration of these features of the method for measuring C_{n_p} led to the design of an alternative arrangement in which the other cross derivative, $C_{l_r}-C_{l_{\dot\beta}}$, was measured. This was done by measuring the rolling moment in a yawing oscillation. This rolling moment includes a contribution from the sideslip derivative C_{l_β} which at high speeds can be several times the magnitude of the moment due to $C_{l_r}-C_{l_{\dot\beta}}$. (The roll axis becomes the z' axis according to the convention of this report, and the moments are apparent from equations (8), (19), and (22) and the direction cosines for a yawing oscillation from the appendix.) Experience with the analog computing system, however, indicated that the accuracy of the system was adequate for separating the damping derivatives from the stiffness derivatives by their difference in phase, and that $C_{l_r}-C_{l_{\dot\beta}}$ could be measured in the presence of the larger moments due to $C_{l_{\dot\beta}}$.

An expanded view of the yawing oscillation mechanism which incorporates a cross-torque gage for measuring $C_{l_r}-C_{l_{\dot\beta}}$ is shown in figure 8. The z', or cross-torque, axis lies along the longitudinal axis of the model. A strain-gage bridge for measuring $\epsilon_{z'}$ was formed consisting of two legs from each of the two unbonded strain gages shown in the photograph. Static tests showed that this gage arrangement eliminated interaction due to forces and moments about all other axes. Subsequent wind-tunnel tests showed that the lateral-directional derivatives could be measured through a wide range of angles of attack without the necessity of trimming the pitching moments. It was found that operation was fairly smooth even at high speeds and angles of attack near the stall. This improved performance was attributed to the fact that there were only slight changes in

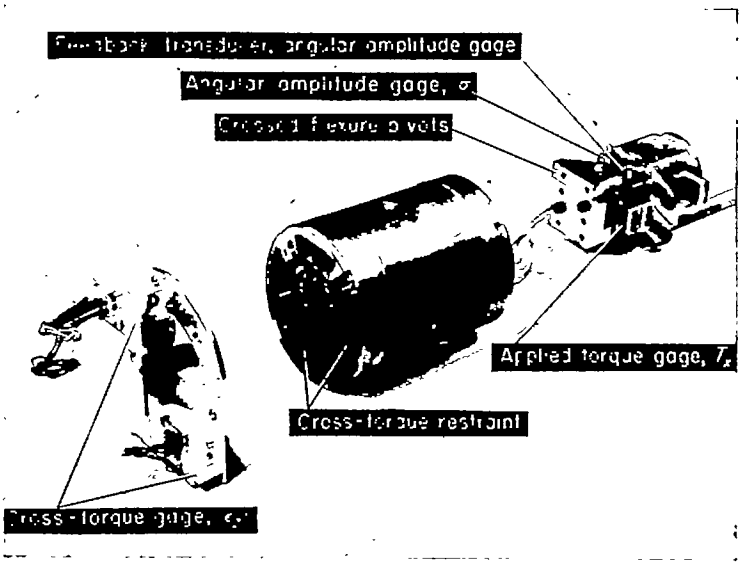

FIGURE 8.—Expanded view of a later version of the oscillation mechanism for yawing or pitching illustrating a more satisfactory method for measuring the cross torque.

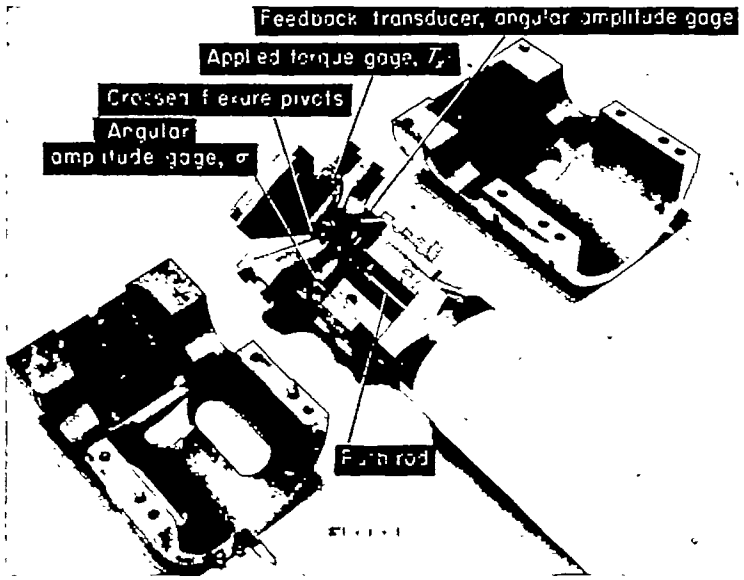

FIGURE 9.—Revised version of the mechanism illustrated in figure 7 in which the cross-torque gage has been eliminated.

effective angle of attack or lift on the wing during a yawing oscillation compared with the larger changes encountered during a pitching or rolling oscillation. This design thus proved to be superior to that shown in figure 7, and, as a result, the cross-torque gage and cross-torque restraint were eliminated from the roll and yaw oscillator as shown in figure 9.

The accuracy of the data obtained with this equipment is believed to be sufficient for most dynamic stability calculations. Errors directly assignable to the computing system are quite small, within 1 percent of the full-scale capacity and 1° of arc in the phase angle. Tare damping caused by friction and other internal effects in the model and mechanism was measured prior to each run, but this measurement was used primarily as an indication of trouble in the equipment since it was normally less than 2 percent of the full-scale capacity and was neglected in computing the derivatives. The vibration characteristics of the sting and supporting system introduced an additional possibility of error which required careful study. Calculated vibration characteristics of the support were used as a guide to evaluate the test conditions under which support vibration might affect the measured results, but these calculations were not found to be reliable because it was difficult to properly account for the various degrees of freedom of the supporting structure. In some cases it was necessary to attach guy wires between the sting and the tunnel wall to prevent the support system from vibrating at the model oscillation frequency and thus introducing errors in the measurements. In most tests, however, these objectionable frequencies were avoided and the results were the same whether the guy wires were attached to the sting or not. Through tests with independent variations in Mach number and Reynolds number, both of which affect the model oscillation frequency, and with the guy wires on and off, it was established that systematic errors due to model support vibration could be eliminated within the random error of the measurements.

The probable random error in a single measurement as a percent of the full-scale damping capacity was found to be less than 1½ percent for both $C_{l'_\sigma}$ and $C_{n'_\sigma}$ from an analysis of repeated measurements on a typical model for Mach numbers from 0.25 up to 0.94 at zero angle of attack. The accuracy of measurement of a single derivative depends on its relation to the maximum value of $C_{l'_\sigma}$. Thus, for conventional airplane models the combined random and systematic uncertainty in a single damping derivative C_{l_p}, $C_{n_r}-C_{n_{\dot\beta}}$, or $C_{m_q}+C_{m_{\dot\alpha}}$ would be of the order of 5 percent, with the cross derivatives, C_{n_p} and $C_{l_r}-C_{l_{\dot\beta}}$, being subject to the same increment of certainty as C_{l_p} and $C_{n_r}-C_{n_{\dot\beta}}$.

EXPERIMENTAL DATA

Figures 10, 11, and 12 have been prepared to illustrate the general scope of data obtainable with the oscillation apparatus described. These data were obtained at a low Mach number for the model configuration illustrated in figure 5. Similar data have been obtained at Mach numbers up to 0.95.

The effects of oscillation amplitude and reduced frequency at a selected angle of attack can be studied from measurements of the type shown in figure 10. It is sometimes desirable to measure only the effect of frequency or amplitude on certain combinations of derivatives, such as $C_{n_p}+C_{l_r}-C_{l_{\dot\beta}}$ in figure 10, since this can be done with fewer measurements. These data confirm the assumption of linearity in the small oscillations of an airplane about an equi-

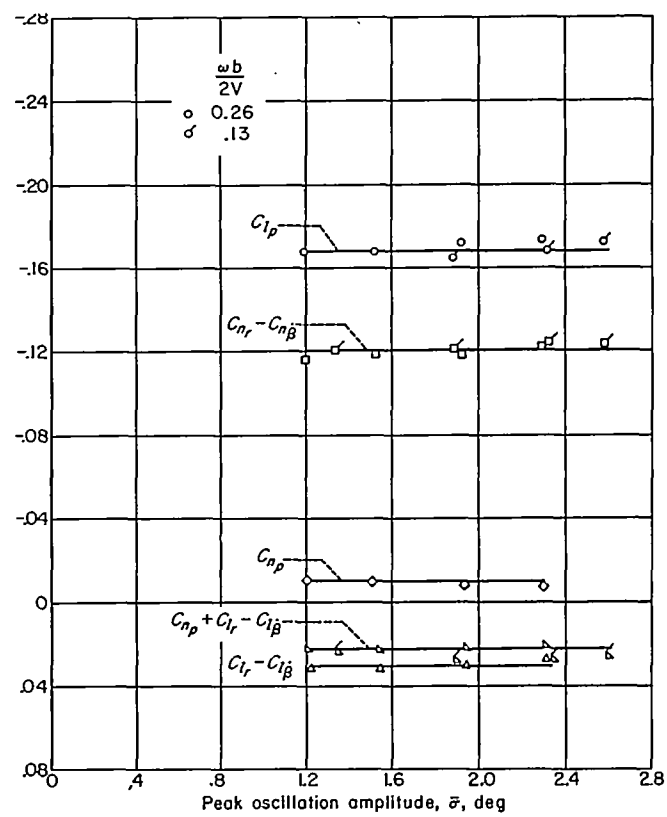

FIGURE 10.—The variation of some of the lateral stability derivatives with oscillation amplitude for two values of reduced frequency.

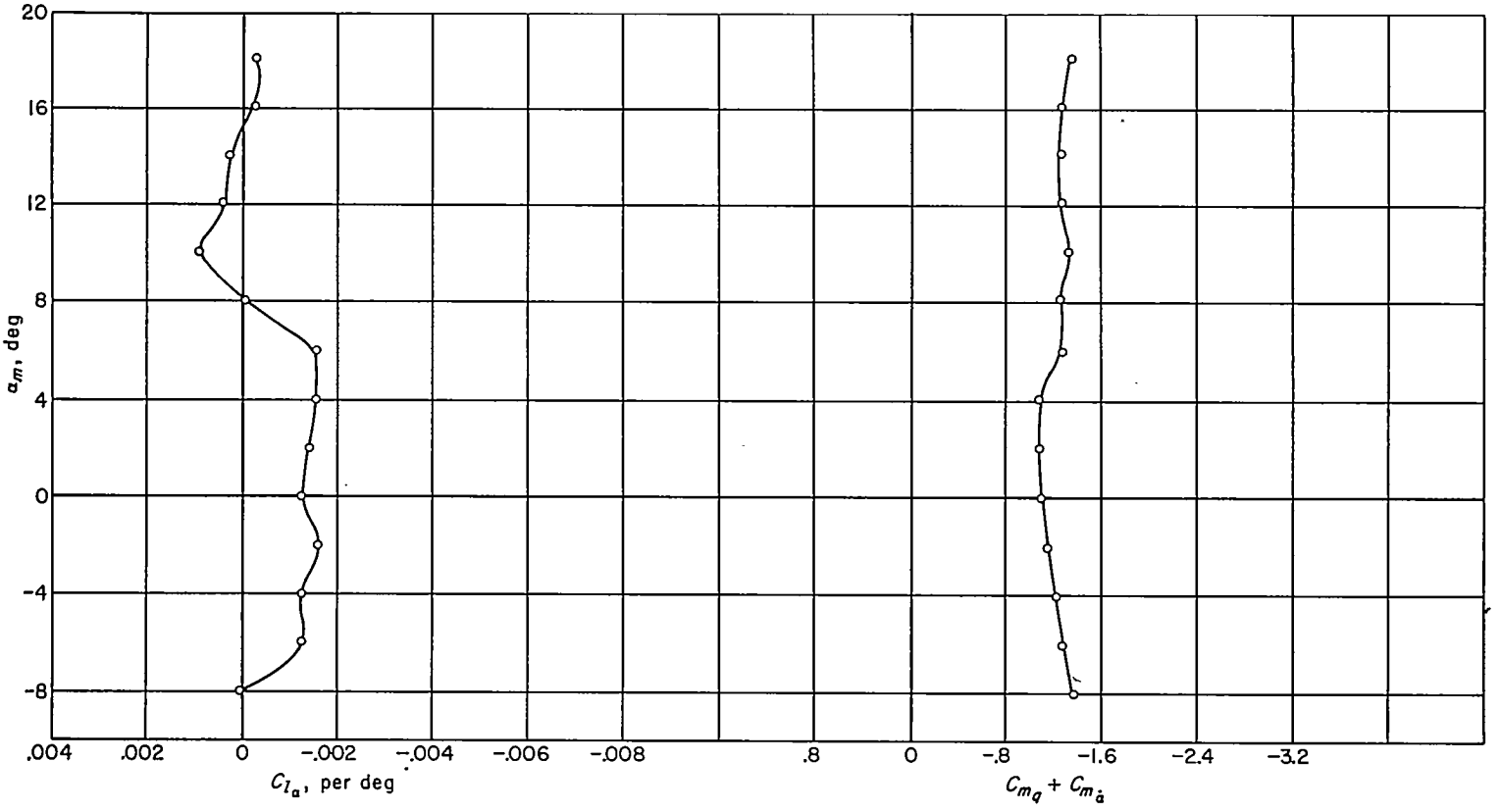

FIGURE 11. The variation of the longitudinal stability derivatives with angle of attack.

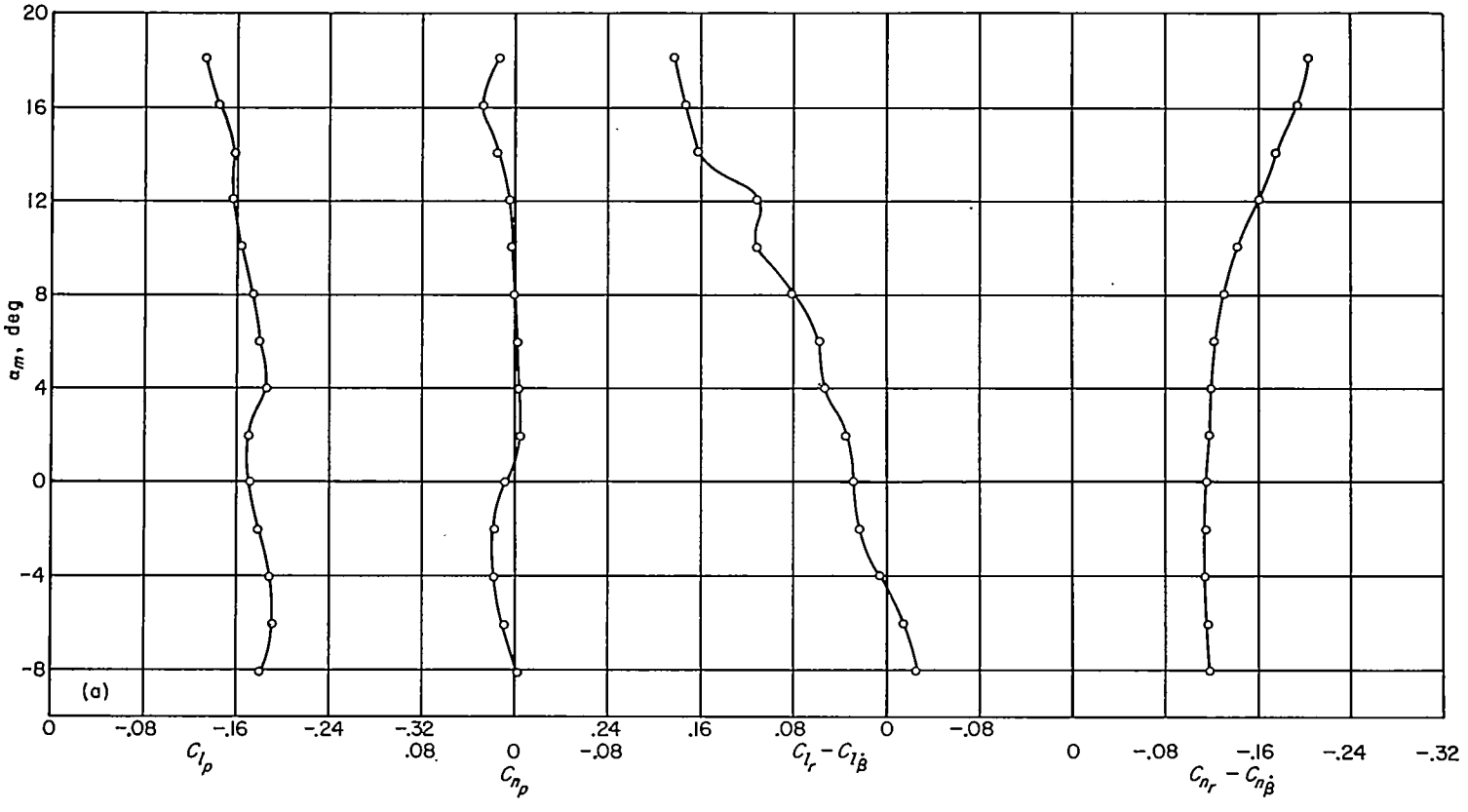

(a) C_{l_p}, C_{n_p}, $C_{l_r} - C_{l_{\dot{\beta}}}$, $C_{n_r} - C_{n_{\dot{\beta}}}$ vs. α_m

FIGURE 12.—The variation of the lateral stability derivatives with angle of attack.

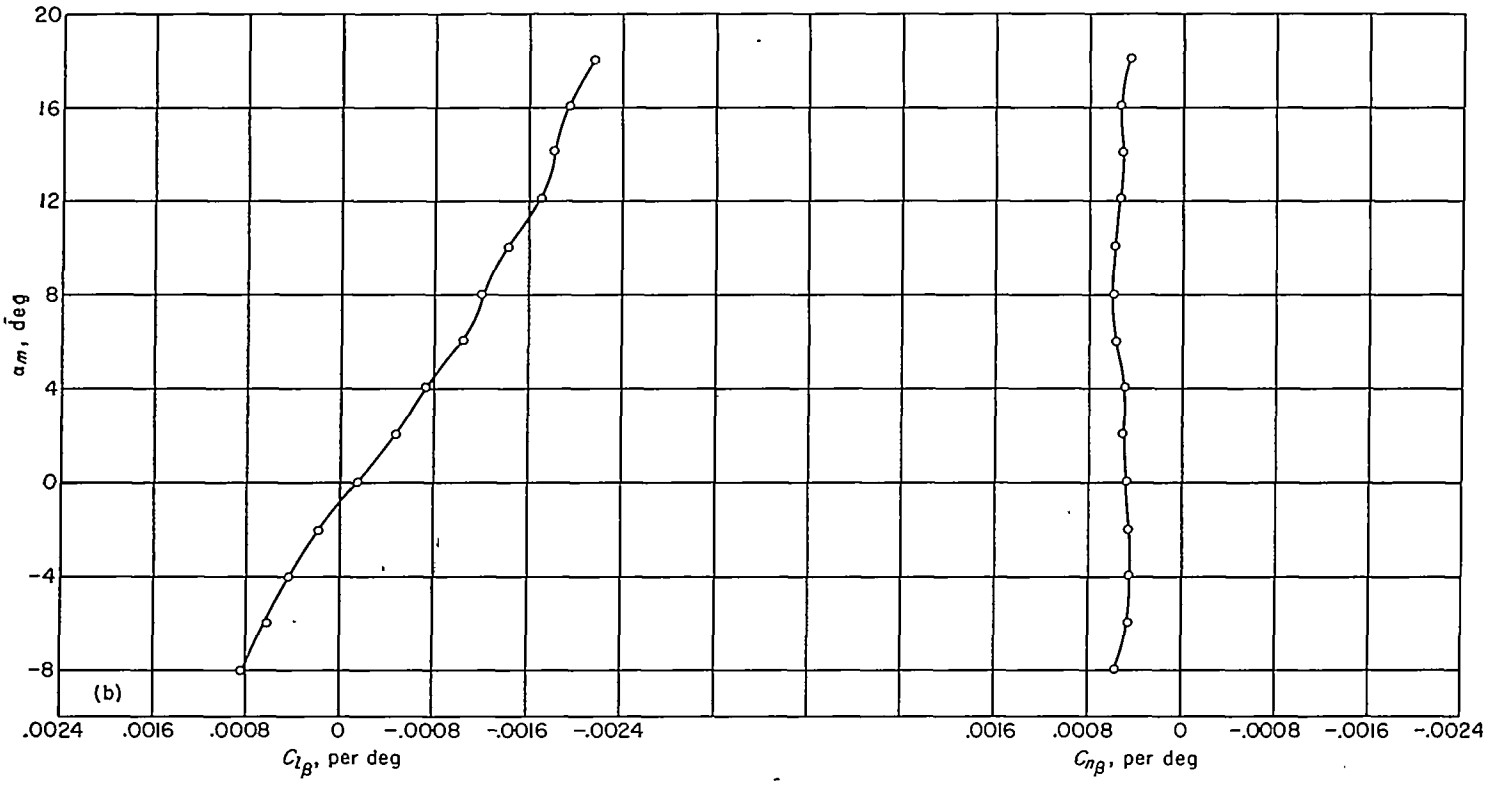

(b) C_{l_β}, C_{n_β} vs. α_m

FIGURE 12.—Concluded.

librium position and indicate that the effects of frequency on the stability derivatives are negligible for the test conditions represented in figure 10.

Data of the type illustrated in figures 11 and 12 can be used to establish the variation of the stability derivatives with angle of attack for a mean oscillation amplitude and frequency as this is the form most useful in dynamic stability calculations. The data shown in figure 11, along with the lift-curve slope, are the aerodynamic parameters of primary importance in estimating the short-period dynamic longitudinal stability of an aircraft with the control surfaces fixed. The short-period motion in this case is essentially a pitching about the center of gravity combined with vertical translation. The desirability of experimentally separating $C_{m_{\dot{\alpha}}}$ and C_{m_q} and evaluating other derivatives which may affect the longitudinal motion depends on the circumstances and on the precision required but, in general, the important features of the motion can be estimated without these additional aerodynamic parameters. In the stick-free case, a third degree of freedom is introduced by the elevator motion about its hinge which may markedly affect the response of the airplane and for which the aerodynamic contribution of the free control surface would have to be considered (ref. 5).

Data of the type illustrated in figure 12 can be used in calculating the dynamic lateral stability of an airplane. Analysis of the lateral oscillatory motion with the controls fixed is more complicated than in the longitudinal case because of the three degrees of freedom—rolling, yawing, and sideslipping. The aerodynamic parameters required, in addition to those shown in figures 12 (a) and (b), are the side-force coefficients due to rolling velocity, yawing velocity, and sideslip (ref. 6). The side force due to sideslip can be measured or estimated from steady-flight considerations alone. Measured values of the side forces due to rolling velocity and yawing velocity would be desirable, but in many cases these forces are small or can be shown to have negligible effect on the motion (ref. 7). Here again, as in the case of the short-period longitudinal motion, free-control surfaces may radically alter the aircraft response (ref. 5).

Many of the suggested methods for calculating dynamic lateral stability (e. g., refs. 5, 6, and 7) do not consider the effects of sideslip velocity $\dot{\beta}$ because, for typical airplane configurations used in the past, these effects have been shown to be small (ref. 3). This may, however, not be the case for current and future airplane types. The effects of $C_{l_{\dot{\beta}}}$ and $C_{n_{\dot{\beta}}}$ on the lateral oscillatory motion can be approximated by introducing the terms $C_{l_r}-C_{l_{\dot{\beta}}}$ and $C_{n_r}-C_{n_{\dot{\beta}}}$ into the equations of motion (ref. 6) in place of C_{l_r} and C_{n_r}. This would indicate that, in the absence of independent measurements of $C_{l_{\dot{\beta}}}$ and $C_{n_{\dot{\beta}}}$, it would be desirable to obtain values of $C_{l_r}-C_{l_{\dot{\beta}}}$ and $C_{n_r}-C_{n_{\dot{\beta}}}$ from oscillation tests since this would approximately account for the possible effects of sideslip velocity in stability calculations.

AMES AERONAUTICAL LABORATORY,
NATIONAL ADVISORY COMMITTEE FOR AERONAUTICS,
MOFFETT FIELD, CALIF., *Sept. 20, 1954.*

APPENDIX

General methods are available for evaluating the direction cosines for an arbitrary rotation of one system of axes with respect to another. (See, e. g., ref. 8.) In the present case it would be most useful if the direction cosines were evaluated in terms of the angles η and λ illustrated in figure 2. The angle η represents the mechanical angle by which the axis of the crossed flexures is offset from the longitudinal axis of the sting and λ is determined by keying the oscillation apparatus to the sting in the proper rotational position. The direction cosines used in equations (17) through (22) then become

$$\left.\begin{aligned} A&=\cos\alpha_m\cos\eta-\sin\alpha_m\sin\eta\cos\lambda\\ B&=\sin\eta\sin\lambda\\ C&=-(\sin\alpha_m\cos\eta+\cos\alpha_m\sin\eta\cos\lambda)\\ D&=\sin\alpha_m\sin\lambda\\ E&=\cos\lambda\\ F&=\sin\lambda\cos\alpha_m\\ G&=\cos\alpha_m\sin\eta+\sin\alpha_m\cos\eta\cos\lambda\\ H&=-\sin\lambda\cos\eta\\ J&=-\sin\alpha_m\sin\eta+\cos\alpha_m\cos\eta\cos\lambda \end{aligned}\right\} \quad (39)$$

In the case of the velocity derivatives, a considerable simplification in the direction cosines can be obtained by referring them to a set of model axes which coincide with the stability axes at zero angle of attack. The velocity derivatives are then evaluated first about model axes for all angles of attack and then transformed to stability axes.

Inserting $\alpha_m=0$ in the above expression for the direction cosines results in the following values for the tests discussed herein, where the double primes refer to model axes:

	Type of motion				
	Pitching	Yawing	Rolling plus pitching[1]	Rolling plus yawing	Rolling minus yawing
η	90°	90°	45°	45°	45°
λ	90°	0	90°	180°	0
A''	0	0	$\frac{1}{\sqrt{2}}$	$\frac{1}{\sqrt{2}}$	$\frac{1}{\sqrt{2}}$
B''	1	0	$\frac{1}{\sqrt{2}}$	0	0
C''	0	−1	0	$\frac{1}{\sqrt{2}}$	$-\frac{1}{\sqrt{2}}$
D''	----	----	0	----	----
E''	----	----	0	----	----
F''	----	----	1	----	----
G''	----	1	----	----	----
H''	----	0	----	----	----
J''	----	0	----	----	----

[1]This mode used only in early tests (see fig. 7).

Use of these values for the direction cosines resulted in the determination of the velocity derivatives about model axes, using equation (17), (18), or (19), as explained in the section on Description of Apparatus. The transformation from model axes to stability axes was made with the following equations where the double-primed coefficients refer to model axes.

$$\left.\begin{aligned} C_{l_p}&=C''_{l_p}\cos^2\alpha_m+\left(C''_{n_r}-C''_{n_{\dot\beta}}\right)\sin^2\alpha_m+\\ &\quad\left(C''_{n_p}+C''_{l_r}-C''_{l_{\dot\beta}}\right)\sin\alpha_m\cos\alpha_m\\ C_{l_r}-C_{l_{\dot\beta}}&=\left(C''_{l_r}-C''_{l_{\dot\beta}}\right)\cos^2\alpha_m-C''_{n_p}\sin^2\alpha_m+\\ &\quad\left(C''_{n_r}-C''_{n_{\dot\beta}}-C''_{l_p}\right)\sin\alpha_m\cos\alpha_m\\ C_{n_p}&=C''_{n_p}\cos^2\alpha_m-\left(C''_{l_r}-C''_{l_{\dot\beta}}\right)\sin^2\alpha_m+\\ &\quad\left(C''_{n_r}-C''_{n_{\dot\beta}}-C''_{l_p}\right)\sin\alpha_m\cos\alpha_m\\ C_{n_r}-C_{n_{\dot\beta}}&=\left(C''_{n_r}-C''_{n_{\dot\beta}}\right)\cos^2\alpha_m+C''_{l_p}\sin^2\alpha_m-\\ &\quad\left(C''_{n_p}+C''_{l_r}-C''_{l_{\dot\beta}}\right)\sin\alpha_m\cos\alpha_m\\ C_{m_q}+C_{m_{\dot\alpha}}&=C''_{m_q}+C''_{m_{\dot\alpha}} \end{aligned}\right\} \quad (40)$$

The displacement derivatives C_{m_α}, C_{n_β}, and C_{l_β} were not evaluated by the above procedure as there was no computational advantage in this case. Equations (17) through (22) are developed about stability axes for which $\beta=-\psi$ and $\alpha=\theta$. The use of these same relations for the model axes system depends on the presence in equations (17) through (19) of the terms due to rolling velocity and the advantage in using the model axes system is that thereby certain terms are eliminated in the equations and simple solutions obtained for all angles of attack. On the other hand, the use of this relation for the displacement derivatives would require the introduction of corresponding terms due to roll deflection about model axes. It can be shown that when these terms are introduced, the resulting equations are as difficult from the computing standpoint as the direct evaluation of the displacement derivatives about stability axes; therefore, in evaluating the displacement derivatives C_{m_α}, C_{n_β}, and C_{l_β}, equation (20) and the direction cosines for the stability system of axes, equation (39), were used.

It is important to note the difference between the model axes system used for equation (40) and the system of body axes used in many stability calculations. The orientation of the two systems of axes coincides but with the body axes system the sideslip angle β is defined as the angle between the relative wind and the plane of symmetry in the same manner as with the stability axes. With the approximations $\sin\sigma=\sigma$, $\cos\sigma=1$, the sideslip angle referred to body axes would become

$$\begin{aligned}\beta&=-\psi''\cos\alpha_m+\varphi''\sin\alpha_m\\ &=(-C''\cos\alpha_m+A''\sin\alpha_m)\sigma\end{aligned}$$

This value for β could be inserted in equations (11), (13), and subsequent equations which would lead to modifications of equations (17) through (22) and these new equations would then represent the stability derivatives referred to body axes. Therefore, while there are many similarities in the two systems, the model axes system used in equation (40) is not a true system of body axes and should be considered only as a computational aid.

REFERENCES

1. Lessing, H. C., Fryer, T. B., and Mead, M. H.: A System for Measuring the Dynamic Lateral Stability Derivatives in High-Speed Wind Tunnels. NACA TN 3348, 1954.
2. MacLachlan, Robert, and Letko, William: Correlation of Two Experimental Methods of Determining the Rolling Characteristics of Unswept Wings. NACA TN 1309, 1947.
3. Bird, John D., Jaquet, Byron M., and Cowan, John W.: Effect of Fuselage and Tail Surfaces on Low-Speed Yawing Characteristics of a Swept-Wing Model as Determined in Curved-Flow Test Section of Langley Stability Tunnel. NACA TN 2483, 1951.
4. Jones, B. Melvill: Dynamics of the Airplane. Symmetric or Pitching Moments. Vol. V of Aerodynamic Theory, div. N, ch. II, sec. 40, W. F. Durand, ed., Julius Springer (Berlin), 1935, pp. 49–50.
5. Phillips, William H.: Appreciation and Prediction of Flying Qualities. NACA Rep. 927, 1949. (Supersedes NACA TN 1670.)
6. Campbell, John P., and McKinney, Marion O.: Summary of Methods for Calculating Dynamic Lateral Stability and Response and for Estimating Lateral Stability Derivatives. NACA Rep. 1098, 1952. (Supersedes NACA TN 2409.)
7. Sternfield, Leonard, and Gates, Ordway B., Jr.: A Simplified Method for the Determination and Analysis of the Neutral-Lateral-Oscillatory-Stability Boundary. NACA Rep. 943, 1949. (Supersedes NACA TN 1727.)
8. Whittaker, Edmund Taylor: A Treatise on the Analytical Dynamics of Particles and Rigid Bodies, with an Introduction to the Problem of Three Bodies. Fourth ed., Dover Pub. (New York), 1944, p. 8.